Results in Physics 6 (2016) 456–460

Contents lists available at ScienceDirect

Results in Physics

journal homepage: www.journals.elsevier.com/results-in-physics

Optimization and spectroscopic studies on carbon nanotubes/PVA nanocomposites

Naziha Suliman Alghunaim

Physics Department, Faulty of Science, King Abdulaziz University, Jeddah, Saudi Arabia

ARTICLE INFO

Article history:
Received 15 July 2016
Accepted 2 August 2016
Available online 8 August 2016

Keywords:
CNTs
XRD
TEM
AC conductivity

ABSTRACT

Nanocomposite films of polyvinyl alcohol (PVA) containing constant ratio of both single and multi-wall carbon nanotubes had been obtained by dispersion techniques and were investigated by different techniques. The infrared spectrum confirmed that SWNTs and MWNTs have been covalently related OH and C—C bonds within PVA. The X-ray diffraction indicated lower crystallinity after the addition of carbon nanotubes (CNTs) due to interaction between CNTs and PVA. Transmission electron microscope (TEM) illustrated that SWNTs and MWNTs have been dispersed into PVA polymeric matrix and it wrapped with PVA. The properties of PVA were enhanced by the presence of CNTs. TEM images show uniform distribution of CNTs within PVA and a few broken revealing that CNTs broke aside as opposed to being pulled out from fracture surface which suggests an interfacial bonding between CNTs and PVA. Maximum value of AC conductivity was recorded at higher frequencies. The behavior of both dielectric constant (ε') and dielectric loss (ε'') were decreased when frequency increased related to dipole direction within PVA films to orient toward the applied field. At higher frequencies, the decreasing trend seems nearly stable as compared with lower frequencies related to difficulty of dipole rotation.

Introduction

Polymer nanocomposites are new materials including two or more phases and one of them is in nano-size [1]. These nanocomposites have recently drawn considerable interest due to the ease with which polymer properties can be modified to achieve characteristics that cannot be performed through a single polymer system. The most difficult task at preparation of nanocomposites is the development of materials with a complete set of desired properties. Nanocomposites can be categorized by their matrix characteristics including nanomaterials, ceramic or polymeric [2–4].

Polymeric nanomaterials have special interest due to combination with appropriate nanofillers like carbon nanotubes (CNTs) that give complexes which are useful for the development of advanced high energy devices, batteries, fuel cells and display devices with ease of fabrication into thin films of desirable sizes. The incorporation of carbon nanotubes into the matrix of polymeric material can markedly influence the properties of polymers. This depends on nature of the type of CNTs and the methods of preparation when it interacts with the chains of polymeric matrix [5–7].

Carbon nanotubes (CNTs) have generated intensive research activities because of their properties that may be exploited for a wide variety of applications [8,9]. The unique properties of CNTs such as electrical conductivity, thermal properties, high strength and aspect ratio have motivated considerable research in incorporating CNTs within polymer to obtain nanocomposites [10–12]. The addition of a small content of CNTs strongly improves the properties of the polymer matrix. So CNT/polymer composites combine the good preparation of the polymers with the excellent properties of the CNTs [13].

Some studies showed a significant improvement of polymer/CNT nanocomposites properties [14,15]. In the present work we prepared polyvinyl alcohol (PVA) doped with low content of both single and multi-walled carbon nanotube by casting technique with the achievement of dramatic enhancement in spectroscopic properties and AC conductivity at room temperature.

Experimental work

Materials

Polyvinyl alcohol (PVA), with the molecular weight of 146000, was obtained from Sigma–Aldrich. Purified single-wall carbon nanotubes (SWCNTs) and multi-wall carbon nanotubes (MWCNTs) were supplied from Nanothinx (Greece). CNTs have an internal

E-mail address: n-al-ghunaim@hotmail.com

http://dx.doi.org/10.1016/j.rinp.2016.08.002
2211-3797/

diameter of nearly 0.8–1.4, length ⩾5 μm and purity 85%. All chemicals were used as received and without purifications.

Preparation

First, 2 g of PVA were placed in a beaker and solubilized in 20 mL of distilled water with stirring at 70 °C continuously for more than 6 h. The obtained solution was then cooled to room temperature for about 3 h. After that, 20 mg of both raw SWCNTs–COOH and MWCNTs–COOH were added to 5 ml distilled water. They were immersed on a beaker for 20 min to give suspension using ultrasonic probe (Eltrosonic type-07). The PVA/SWCNTs and PVA/MWCNTs nanocomposites were prepared by the following procedure. Solutions of SWCNTs–COOH and MWCNTs–COOH suspension were added dropwise to PVA solution with stirring continually. Finally, CNTs/PVA nanocomposites were cast in Petri dishes and left in an oven at 60 °C to dry for about 72 h.

Measurements

An FT-IR spectrophotometer (Nicolet iS10, USA) was used to obtain IR spectra. The spectra of IR were collected in wavenumber from 4000 to 400 cm^{-1}. The X-ray diffraction of these samples was recorded on a SIEMENS D5000 diffractometer with CuKα radiation at $\lambda = 0.15406$ nm, Bragg angle (2θ) in the range of 10–55°. Transmission Electron Microscope (TEM), (JEOL-JEM-1011, Japan) was used to study size, shape and distribution of nanoparticles inside polymer matrices. The AC electrical properties were studied by utilizing programmable automatic (Model Hioki 3531Z Hitester) analyzing to measure loss tangent ($\tan\delta$), capacitance C and impedance Z with the frequencies from 100 Hz to 5 MHz.

Results and discussion

Fourier transform infrared spectroscopy (FT-IR)

The FT-IR spectra of pure PVA, SWCNTs/PVA, and MWCNTs/PVA nanocomposites are shown in Figs. 1a, 1b in the range of (4000–500 cm^{-1}). For pure PVA, the characteristic absorption bands are at 3527 cm^{-1} (OH stretching), 3090 cm^{-1} (CH_2 asymmetric stretching), 2878 cm^{-1} (CH_2 symmetric stretching), small new bands appeared at 3468 cm^{-1} and 2928 cm^{-1}, 1737 cm^{-1} (C═O), 1655 cm^{-1} (C═C), 1373 cm^{-1} (CH_2 wagging), 1330 cm^{-1} (CH bending), 1240 cm^{-1} (CH wagging), 1141 cm^{-1} (C—C and C—O—C stretching), 1058 cm^{-1} (C═O stretching), 1031 cm^{-1} (C—O stretching), 916 cm^{-1} (CH_2 Rocking), and 850 cm^{-1} (C—C stretching) (see Table 1) [16,17].

Table 1
The assignment of IR bands of pure PVA films at room temperature.

Wavenumber (cm^{-1})	Assignment
3527	OH stretching
3090	CH_2 asymmetric stretching
2980	CH_2 symmetric stretching
1736	C═O
1655	C═C
1373	CH_2 wagging
1330	(CH—OH) bending
1241	CH wagging
1141	C—C and C—O—C stretching
1096	C═O stretching
1031	C—O stretching
916	CH_2 Rocking
850	C—C stretching

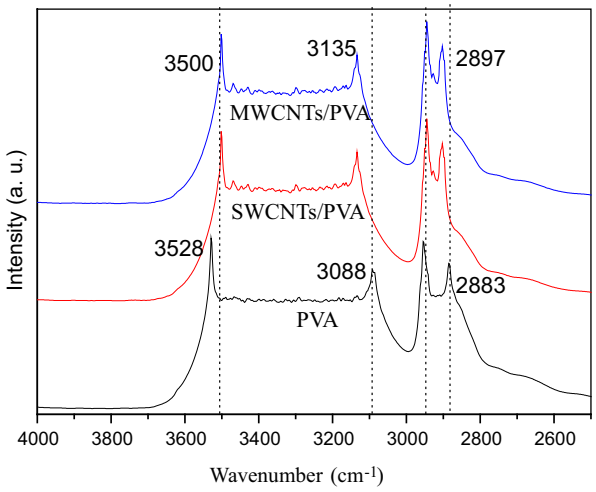

Fig. 1a. IR spectra of PVA, SWCNTs/PVA and MWCNTs/PVA nanocomposites in the range from 4000 to 2500 cm^{-1}.

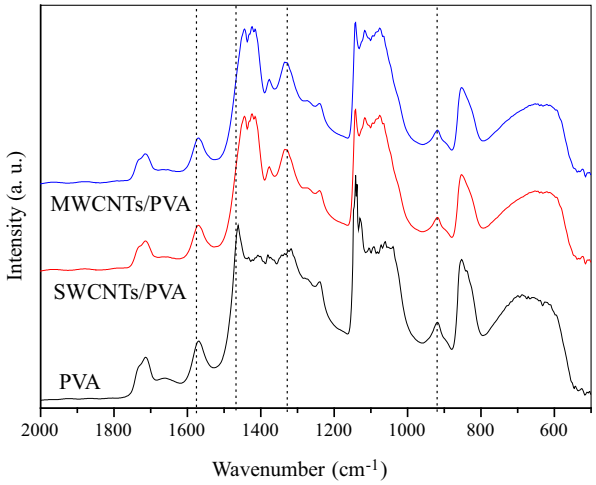

Fig. 1b. The FT-IR spectra of PVA, SWCNTs/PVA and MWCNTs/PVA nanocomposites in the range from 2000 to 500 cm^{-1}.

For the spectrum of PVA doped CNTs, as seen in Fig. 1a, the following are observed: In the range of 4000–2500 cm^{-1}, small new bands appeared at 3468 cm^{-1} and 2928 cm^{-1} attributed to COOH coming during functionalization of CNTs and the band at 3527 cm^{-1} was shifted to 3500 cm^{-1} (with an increase in the its intensity); the band at 3090 cm^{-1} was shifted to 3134 cm^{-1}; the band at 2953 cm^{-1} was shifted to 2944 cm^{-1}; the band at 2883 cm^{-1} was shifted to 2904 cm^{-1} and small new bands appeared at 3468 cm^{-1} and 2928 cm^{-1} respectively. Therefore, the spectrum evidences the presence of carboxyl groups. The shift of lower frequency may be due to open of π-bonds of CNTs and interactions between CNTs and PVA polymeric matrixes.

In the range of 2000–500 cm^{-1}, as seen in Fig. 1b, a new band appeared at 1422 cm^{-1}. A new small broad band at 1655 cm^{-1} is attributed to C—C band between CNTs and PVA. The appearance of this band might be the signature for interaction of π-bonds at the surface of CNTs with the open double band on PVA. The intensity of the band at 1144 cm^{-1} was decreased. The band at 1058 cm^{-1} was shifted to 1074 cm^{-1} with increasing of the intensity. The intensity of the band at 850 cm^{-1} was decreased. The decrease in the intensity for these bands may be due to the strength of stretching vibration of C—C and/or C—O—C bonds composing six carbon rings at the surface of CNTs. It can be seen that

the change of MWCNTs/PVA spectrum is nearly similar to those changes in SWCNTs/PVA spectrum.

X-ray diffraction analysis

Fig. 2 represents the X-ray diffraction of pure PVA, SWCNTs/PVA and MWCNTs/PVA nanocomposites. A peak at $2\theta = 19.71^\circ$ ascribed to pure PVA [18,19] has been observed, this peak corresponds to (110) reflection. An increase in broadness and decrease in peak intensity have been observed within the samples that contain CNTs. This reveals the amorphous nature of the new material which means an increase in the degree of crystallinity.

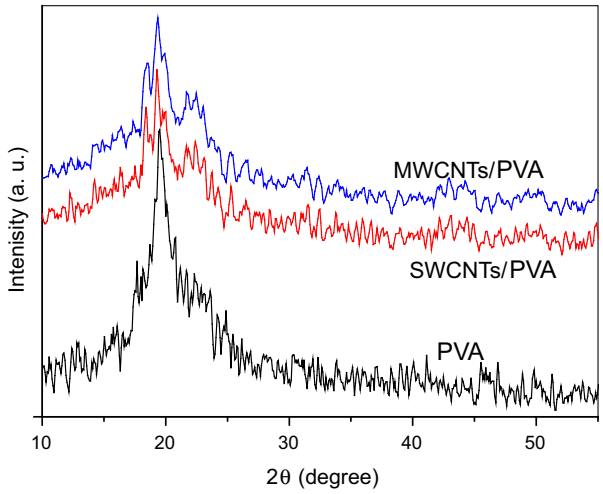

Fig. 2. X-ray diffraction scans of PVA, SWCNTs/PVA and MWCNTs/PVA nanocomposites.

Change of peak intensity has been found in the samples doped CNTs indicating a complete dissociation of CNTs in the polymer matrix. In general, the crystalline nature of PVA was detected from strong interaction between PVA through intermolecular hydrogen bonding. An interaction between PVA with carboxylic group (COOH) in CNTs led to the decrease in intermolecular interaction of PVA chains, which results in the decrease in the degree of PVA-crystalline. New peak corresponding to different crystal planes which indicates the reflections that correspond to CNTs at $2\theta \sim 26.48^\circ$ was observed. This peak is corresponding to the (002) reflection of hexagonal crystal structure of graphite.

TEM morphology

Fig. 3 indicates the TEM images results of pure PVA, SWCNTs/PVA, and MWCNTs/PVA with different magnifications. It is observed that CNTs were implanted uniformly within the PVA matrices and have intimate contact with these polymeric matrices. Broken of some CNTs ends had been observed, revealing that CNTs broke aside in place of being pulled out from the fracture surface, which suggests the existence of strong interfacial bonding among CNTs and PVA. Also, PVA form a masking layer on CNTs/PVA images, showing that some defects like ragged or worm eaten at

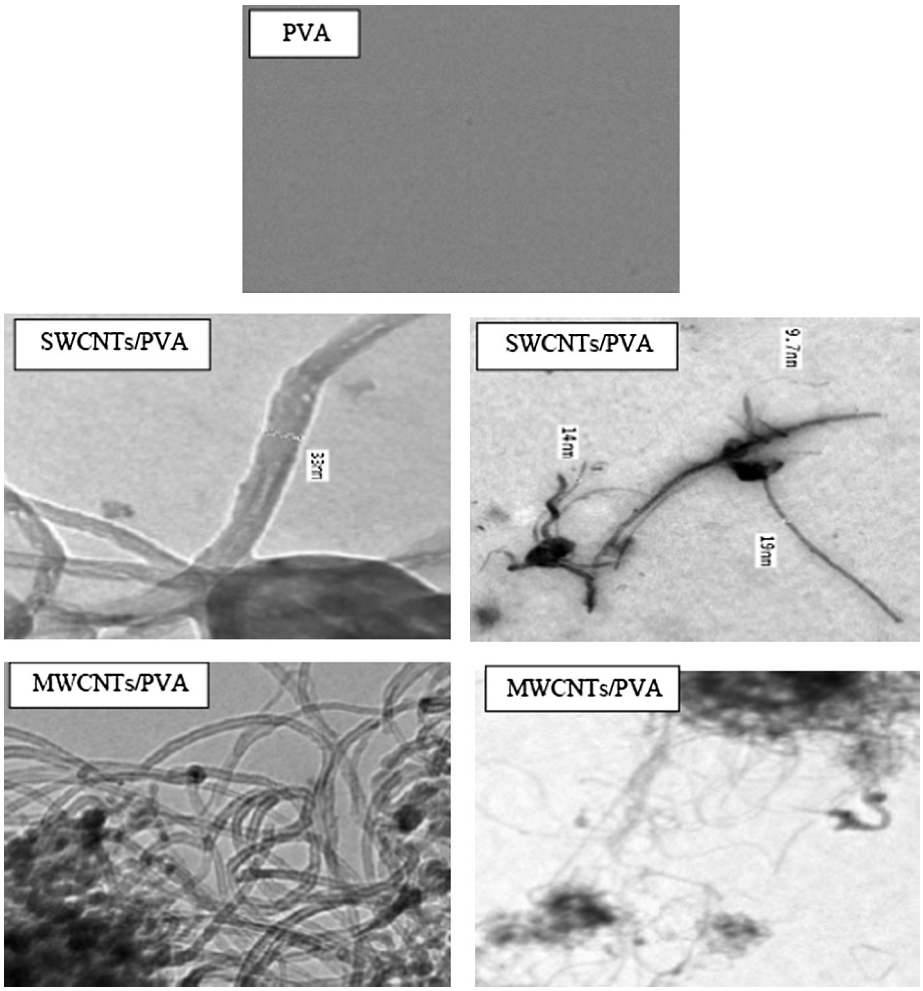

Fig. 3. TEM images of PVA, SWCNTs/PVA and MWCNTs/PVA nanocomposites.

tube walls and partitions with buckles and irreversible bends, which are the effect of chemical processing. The presence of these defects increases the interaction sites along the tubes with PVA. Moreover, SWCNTs and MWCNTs were arranged in different diameters ranging 8–16 nm and length up to 10 μ and wrapped with PVA. This is very useful in technical application. There are a few black regions due to the amorphous nature of carbon.

Electrical conductivity

Fig. 4 represents the AC conductivity of PVA without and with CNTs in frequencies ranging 100 Hz–5 MHz at room temperature. The AC conductivity was estimated from the equation [20],

$$\boldsymbol{\sigma} = \frac{L}{RA} \tag{1}$$

where L is thickness, R is resistance of the sample and A is cross section area of electrode.

Generally, the behavior of AC conductivity of pure polymer shows that the frequency dependence is due to the insulating nature of polymer material but it is significantly changed after addition of CNTs which exhibits frequency independence as well as the value was improved several orders of magnitude. The highest value of AC conductivity was recorded at maximum frequency (5 MHz) and when adding MWCNTs than SWCNTs. It can be attributed that effective conductive network is formed when CNTs loading in polymer according to the percolation theory according to impurity contributions arising from CNTs, where molecules of CNTs begin to bridge gap separated between localized states and potential barrier thereby facilitating charge carrier transfer. Then, doped samples are a good candidate to obtain semiconducting organic nanocomposites.

The electrical parameters (dielectric constant, ε' and dielectric loss, ε'') were calculated using Phase Sensitive LCR meter. The dielectric constant (ε') was estimated from the relation [21,22]:

$$\varepsilon' = \frac{C.d}{\varepsilon_o.A} = \frac{\varepsilon''}{\tan\delta} \tag{2}$$

where C is capacitance, d is thickness of the films and ε_o is the permittivity of free space ($\varepsilon_o = 8.85 \times 10^{-12}$ F/m).

The dielectric constant (ε') depends on the frequency (Log f) for the prepared samples is seen in Fig. 5. It can be seen that the dielectric constant was decreased when the frequency increased for all samples due to the direction of dipoles within polymeric films to orient in the direction of applied field. But at higher frequencies, the decreasing trend of dielectric constant seems not sharp (nearly stable) as compared with lower frequencies. This trend may be attributed to dipole orientation, making it difficult to rotate the dipoles at high frequencies. Furthermore, at low frequencies, the values of permittivity are high due to the interfacial effect of nanocomposite films and electrode effect [23].

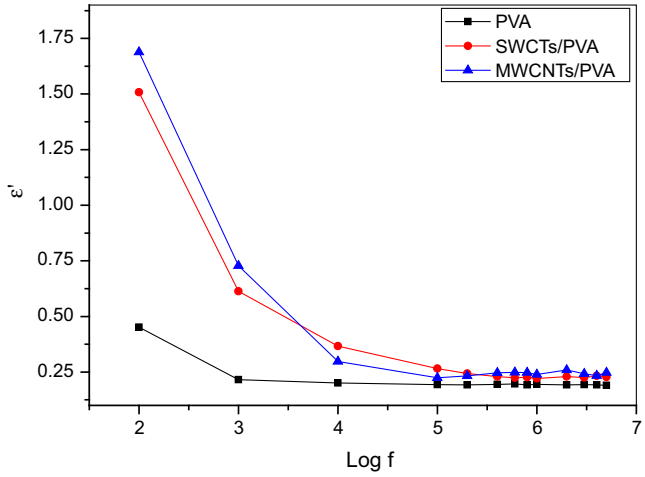

Fig. 5. The dielectric constant (ε') depends on frequency (Log f) of PVA with SWCNTs and MWCNTs.

Fig. 6 depicts the dielectric loss (ε'') depends on the frequency (Log f) for the prepared samples. The dielectric loss was increased after the addition of CNTs, which indicates the higher charge carrying capacity of loaded films compared to pure PVA film. The maximum values of dielectric loss were recorded at low frequencies due to the mobile charges within the polymer backbone. The maximum value of the dielectric loss at higher content of CNTs may be understood in terms of electrical conductivity. In general, the mobile charges (polarons and/or bipolrons) that belong to conducting polymer and free charge increase at addition of the CNTs cause influence and the lower values of ε'' at high frequencies [24].

The relation between loss tangent ($\tan\delta$) depends on frequency (Log f) of the samples is shown in Fig. 7. From the figure, the loss tangent for all films decreases with increasing frequency. The higher value of $\tan\delta$ was observed at low frequency in all films. After the addition of CNTs, it is expected because the conductivity increases with increase in CNTs [25]. If hopping frequency is

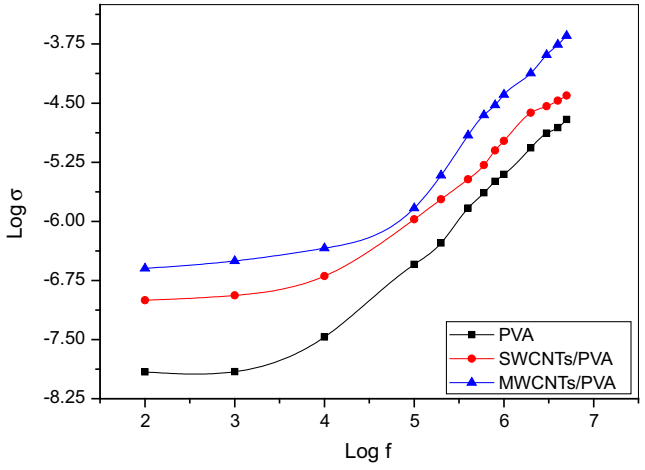

Fig. 4. The AC conductivity of PVA with SWCNTs and MWCNTs.

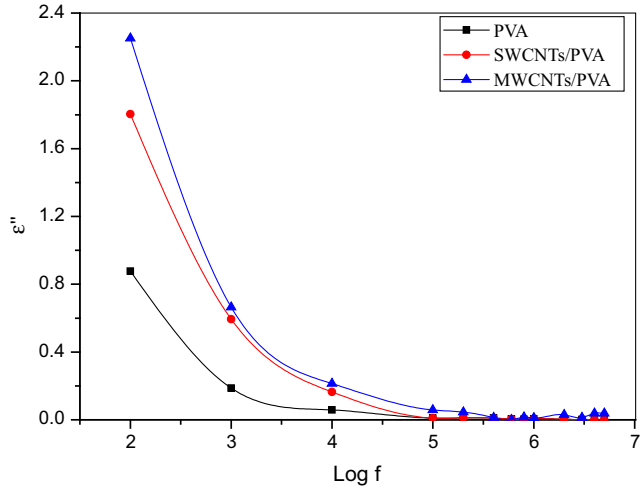

Fig. 6. The dielectric loss (ε'') depend on frequency (Log f) of PVA with SWCNTs and MWCNTs.

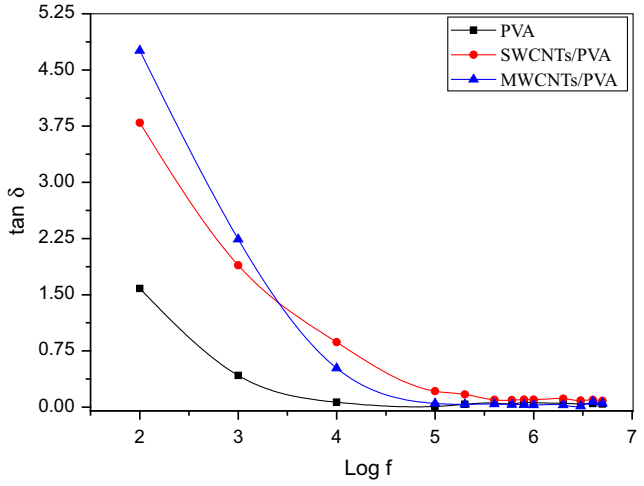

Fig. 7. The variation of loss tangent (tan δ) with frequency (Log f) of PVA with SWCNTs and MWCNTs.

almost equal to the frequency of external applied field, then maximum values of loss tangent were determined. The decrease in tan δ with increasing frequency is due to the fact that the hopping frequency of charge carriers cannot follow the changes of this applied field on the far side an exact limitation of the frequency [26,27].

Conclusions

Films of PVA doped single and multi-walled carbon nanotubes were studied. The decrease in some IR bands is due to the strength of vibration bonds composing six carbon rings at the surface of CNTs. An increase in broadness in X-ray spectra with decrease in peak intensity reveals the amorphous nature of the samples. New peaks were found after doped CNTs indicating a complete dissociation of CNTs in PVA matrix. New peak corresponds to crystal plane reflections of hexagonal structure. TEM images show that CNTs were implanted uniformly within PVA. More ends of CNTs broken revealing that CNTs broke apart than being pulled out from fracture surface indicate strong interfacial bonding between CNTs and PVA. The highest value of AC conductivity was recorded at 5 MHz attributed effective conductive network formed when CNTs loading according to percolation theory. Molecules of CNTs worked bridge gap separated between two localized states and potential barrier. The dielectric constant was decreased when the frequency increases due to dipole direction within polymeric films to orient toward the applied field. At higher frequencies, the decreasing trend of dielectric constant seems not sharp (nearly stable) as compared with lower frequency attributed to dipole orientation making it difficult to rotate dipoles at high frequencies. Maximum values of ε'' were observed at lower frequencies due to mobile charges within PVA backbone. The highest value of AC conductivity and AC parameters were recorded for the samples doped MWCNTs than PVA/SWCNTs.

References

[1] Camaro PHC, Satyanarayana KG, Wypych F. Mater Res 2009;12:1.
[2] Hossen MF, Hamdan S, Rahman MR, Islam MS, Liew FK, Lai JC, Rahman MM. Measurement 2016;90:404.
[3] Zare Y. Compos Part A: Appl Sci Manuf 2016;84:158.
[4] Chen C, Wang H, Xue Y, Xue Z, Liu H, Xie X, Mai Y. Compos Sci Technol 2016;128:207.
[5] Jeon HG, Jung HT, Lee SW, Hudson SD. Polym Bull 1998;41:107.
[6] Okamoto M, Morita S, Kotaka T. Polymer 2001;42:2685.
[7] Yao KJ, Song M, Hourston DJ, Luo DZ. Polymer 2002;43:1017.
[8] Iijima S. Nature 1991;354:56.
[9] Iijima S, Ichihashi T. Nature 1993;363:603.
[10] Aqela A, Abou El-Nour KMM, Ammar RAA, Al-Warthan A. Arab J Chem 2012;5:1.
[11] Du JH, Bai J, Cheng HM. eXPRESS Polym Lett 2007;5:253.
[12] Chen WX, Tu JP, Wang LY, Gan HY, Xu ZD, Zhang XB. Carbon 2003;41:215.
[13] Cadek M, Coleman JN, Barron V, Hedicke K, Blau WJ. Appl Phys Lett 2002;81:5123.
[14] Sandler J, Shaffer MSP, Prasse T, Bauhofer W, Schulte K, Windle AH. Polymer 1999;40:5967.
[15] Shaffer MSP, Windle AH. Adv Mater 1999;11:937.
[16] Abd El-Kader FH, Gaafer SA, Abd El-Kader MFH. Spectrochim Acta Part A Mol Biomol Spectrosc 2014;131:564.
[17] Elashmawi IS, Abdelghany AM, Hakeem NA. J Mater Sci: Mater Electron 2013;24:2956.
[18] Elashmawi IS, Abdel Baieth HE. Curr Appl Phys 2012;2:141.
[19] Lee YM, Kim SH, Kim SJ. Polymer 1996;37:5897.
[20] Nigrawal A, Chand N. Int J Eng Sci Technol 2012;4:191.
[21] Jobish J, Charoen N, Praveen P. J Non-Crystal Sol 2012;358:1113.
[22] Abdelaziz M, Ghannam MM. Phys B 2010;405:958.
[23] Bharati A, Wübbenhorst M, Moldenaers P, Cardinaels R. Macromolecules 2016;49:1464.
[24] Mohamed SA, Al-Ghamdi AA, Sharma GD, El Mansy MK. J Adv Res 2014;5:79.
[25] Kodgire PV, Bhattacharyya AR, Bose S, Gupta N, Kulkarni AR, Misra A. Chem Phys Lett 2006;432:480.
[26] Ravinder D, Vijaykumar K. Bull Mater Sci 2001;5:505.
[27] Rezlescu N, Prakash C, Prasad G. J Phys D: Appl Phys 2006;39:1635.